Thermodynamic Description of Ternary FE-X-P Systems. Part 4: FE-MO-P

J. Miettinen, A. Pashkova, and G. Vassilev

Thermodynamic descriptions of the Fe-Mo-P system and its binary sub-system, Mo-P, are developed in the frame of a new Fe-X-P (X = Al, Cr, Cu, Mn, Mo, Nb, Ni, Si, Ti) database. The thermodynamic parameters of the binary sub-systems, Fe-Mo and Fe-P, are taken from earlier assessments (modifying slightly the Fe-Mo description) and those of the Fe-Mo-P and Mo-P systems are optimized in this study using experimental thermodynamic and phase equilibrium data available in the literature. The solution phases (i.e., bcc_A2, fcc_A1, Liquid) are described with the substitutional solution model. The binary compounds: Fe_2Mo, FeP, Mo_3P and MoP, are treated as stoichiometric phases, while for Fe_3P and Fe_2P two-sublattice models accounting for the dissolution of Mo were applied. Some intermetallic compounds (Mu, R and Sigma) are described with three-sublattice models.

1. Introduction

The current paper continues an earlier started project[1–3] for the development of a Fe-X-P database. The aim is to design a simple and compatible thermodynamic database, which provides important and practical input data for thermodynamic-kinetic models simulating the solidification of phosphorous steels.[4]

The binary thermodynamic data retained from the literature are these of Andersson[5] (mainly) for the Fe-Mo system, and from Shim et al.[6] and Miettinen and Vassilev[1]—for the Fe-P system. We would like to emphasize that the latter optimization has been implemented by Shim et al.[7] to the very important system Fe-P-C as well. Thus, the current database would be compatible with the a.m. assessment.

The Fe-P system was optimized by Ohtani et al.[8] as well, using the first principle calculation of the enthalpy of formation of the Fe-P intermetallics (the Fe-P optimization of Shim et al.[6] (already published at that time) was not mentioned neither discussed by those authors[8]). However, Changjun et al.[9] reported that the thermodynamic parameters of Ohtani et al.[8] "may underestimate the Gibbs

energy of the Fe_3P phase while may over-estimate that of the Fe_2P phase". For this reason, these authors[9] have retained the Fe-P parameters of Gustafsson[10] used in the optimization of the Fe-Mo-P system. Anyhow, that description could not be directly adapted for the needs of the current database.

Thus, the goal of this work is to achieve new thermodynamic optimizations of the ternary Fe-Mo-P system and its binary sub-system Mo-P. The thermodynamic description of the Fe-Mo system had to be partially modified as well, in order to get a better fit for some solid-liquid equilibria in this as well as in other ternary systems (Fe-Cr-Mo, Fe-Mo-Ni and Fe-Mo-Si).

2. Phases, Modeling and Data

Detailed descriptions of the substitutional solutions and sublattice models and their parameters are available from Lukas et al.[11] Thus, a summary of the phases and the models used in this work is presented in Table 1.

The solution phases (i.e. bcc_A2, fcc_A1, Liquid) are modeled with the substitutional solution model (Table 1). Most of the binary compounds: Fe_2Mo, FeP, Mo_3P and MoP, are treated as stoichiometric phases, while for Fe_3P and Fe_2P two-sublattice models accounting for the dissolution of Mo were applied.

Some intermetallic compounds (Mu (μ), R and Sigma (σ)) are described with three-sublattice models. One should be aware that the maximum dissolution of 10 wt.%Mo in FeP and 5 wt.% Fe in MoP, reported by Guerin and Sergent,[12] at 800 °C, was not considered. This simplifies the calculations but the main reason is the lack of corresponding data at other temperatures and also the lack of any phase equilibrium experimental information for the regions situated along or nearby the FeP-MoP section line.

The studies on the Fe-Mo-P system, up to 1988, have been reviewed by Raghavan.[13] The experimental information selected in the current work for the optimization of the

J. Miettinen, School of Chemical Technology, Aalto University, Espoo, Finland; **A. Pashkova,** DECHEMA-Forschungsinstitut SbR, 60486 Frankfurt am Main, Germany; and **G. Vassilev,** Faculty of Chemistry, University of Plovdiv, 24 Tsar Asen str, 4000 Plovdiv, Bulgaria. Contact e-mail: gpvassilev@gmail.com.

Mo-P and the Fe-Mo-P systems is compiled in Table 2. In addition, topological data about the Fe-Mo phase equilibria,[20–28] the integral molar mixing enthalpy values of the Fe-Mo liquid solutions from Iguchi et al.[29] and the Fe-activity in liquid Fe-Mo alloys from Ichise et al.[27] are used for the partial re-optimization of the Fe-Mo system done is this work.

3. Results

The liquid Fe-Mo phase description by Andersson[5] was modified in this work in order to improve the agreement between the calculated and the experimental (bcc + L)-region of the system. The system Mo-P was reoptimized using the available literature experimental data (Table 2).

The adjustable parameters of the Fe-Mo-P system, obtained in the current study, are presented in Table 3. The parameters marked with a reference code were adopted from earlier assessments. Those marked with O or E were optimized or estimated in this work as follows: O—the parameter was optimized using literature experimental data

(Table 2); E—the parameter was estimated taking into account the relative stabilities of the corresponding phases and keeping realistic values of their integral and partial thermodynamic quantities.

The Gibbs energy expressions for the phases Fe_3P, Fe_2P and FeP, given by Shim et al.,[6] have already been simplified[1,2] by changing the reference states of Fe and P. In this work we keep the modified versions. There are no significant differences between the results of the calculations done in both ways.

In order to verify the current optimizations, the calculated results have been compared with the original experimental data by making use of the ThermoCalc software.[32] Thus, Fig. 1 through 3 show the Fe-Mo and the Mo-P phase diagrams, whose parameters were modified in the current study, and the Fe-P phase diagram calculated by Ref 1,6. The agreements with the experimental data are good.

The new liquid phase description of the Fe-Mo system (Fig. 1) yields solid-liquid equilibria, which only slightly deviate from those of Andersson.[5] Nevertheless, in Fig. 4 one can see that (bcc + L)-region shows improved agreement with the experimental data of Gibson et al.[21] That new description also fits better for describing the phase equilibria in the ternary Fe-Cr-Mo, Fe-Mo-Ni and Fe-Mo-Si systems, allowing the usage of some lower-value ternary liquid-state parameters in these descriptions (to be published). For the integral molar mixing enthalpy and the liquid phase Fe-activity, the current results are quite similar to those of Andersson,[5] agreeing reasonably well with the experimental data of Ichise et al.[27] and Iguchi et al.[29]

Figures 5 through 14 and Table 4 contain the results of the calculations for the Fe-Mo-P system, together with the selected experimental data (Table 2). The agreement is rational and in most cases, it is slightly better than that obtained by Gustafsson.[7]

The liquidus projection of the system (Fig. 5) shows different representation of the reactions concerning codes U_1 and E_1 (Table 4). No suggestions based on experimental data have been given for the invariant points at high Mo contents. The current calculations and those of Gustafsson,[7] however, yield quite similar primary surfaces for the system.

In the vertical sections (Fig. 6 through 11) and the isothermal sections (Fig. 12, 13), reasonable agreement between the current calculations and the experimental data of Vogel and Horstmann,[14] Kaneko et al.[15] and

Table 1 Phases and their modeling in the present Fe-Mo-P description

Phase	Modeling
Liquid (L)	(Fe,Mo,P), substitutional, RKM
bcc_A2 (bcc)	(Fe,Mo,P), substitutional, RKM
fcc_A1 (fcc)	(Fe,Mo,P), substitutional, RKM
Mu (μ)	$(Fe)_7(Mo)_2(Fe,Mo)_4$, sublattice, RKM
R	$(Fe)_{27}(Mo)_{14}(Fe,Mo)_{12}$, sublattice, RKM
Sigma (σ)	$(Fe)_8(Mo)_4(Fe,Mo)_{18}$, sublattice, RKM
Fe_3P (dissolving Mo)	$(Fe,Mo)_3(P)$, sublattice, RKM
Fe_2P (dissolving Mo)	$(Fe,Mo)_2(P)$, sublattice, RKM
Fe_2Mo (λ)	$(Fe)_2(Mo)$, stoichiometric
FeP	(Fe)(P), stoichiometric
Mo_3P	$(Mo)_3(P)$, stoichiometric
MoP	(Mo)(P), stoichiometric
white_P (whi)	(P)

RKM: Redlich–Kister–Muggianu expression (excess Gibbs energy model)

Table 2 Experimental data applied in the optimization for the Mo-P and Fe-Mo-P systems

System	Experimental data	Reference
Fe-Mo-P	Liquidus projection	Vogel and Horstmann[14]
	6 Vertical sections, at Fe-MoP, at 5, 10 and 15 wt.% P, and at 5 and 10 wt.% Mo	Vogel and Horstmann[14]
	Isothermal section, at 800 °C	Kaneko et al.,[15] Raghavan[13]
	Activity coefficient(a) γ_P^{Mo} in liquid, at 1400 and 1600 °C	Yamada and Kato,[16] Ban-Ya et al.,[17] Ueno et al.[18] (theoretical)
Mo-P	Topological data about the phase equilibria	Brewer and Lamoreaux[19] (suggested)

(a) The symbol γ_P^{Mo} describes the effect of the Mo-content on the P activity coefficient, and is defined as $\gamma_P^{Mo} = \gamma_P^{(Fe-Mo-P)} / \gamma_P^{(Mo-P)}$ (where the P content is fixed)

Table 3   Thermodynamic description of the Fe-Mo-P system

	Reference
Liquid (1 sublattice, sites: 1, constituents: Fe,Mo,P)	
$L_{Fe,Mo}^{L} = (-6900 - 0.23T) + (-9000 + 3.85T)(x_{Fe} - x_{Mo})$	O*
$L_{Fe,P}^{L} = (-216,603 + 47.028T) + (-12,490 - 6.749T)(x_{Fe} - x_{P}) + (+43,546)(x_{Fe} - x_{P})^2$	[6]
$L_{Mo,P}^{L} = (-206,000)$	O*
$L_{Fe,Mo,P}^{L} = (+100,000)x_{Fe} + (+100,000)x_{Mo} + (-100,000)x_{P}$	O*
bcc (1 sublattice, sites: 1, constituents: Fe,Mo,P)	
$L_{Fe,Mo}^{bcc} = (+36,818 - 9.141T) + (-362 - 5.724T)(x_{Fe} - x_{Mo})$	[5]
$L_{Fe,P}^{bcc} = (-182,800 + 25.6T)$	[1]
$L_{Mo,P}^{bcc} = (-197,000)$	O*
$L_{Fe,Mo,P}^{bcc} = (+200,000)$	O*
$Tc^{bcc} = 1043x_{Fe} + x_{Fe}x_{Mo}(335 + 526(x_{Fe} - x_{Mo})) - 1100x_{Fe}x_{P}$	[1,5]
$\beta^{bcc} = 2.22x_{Fe}$	[5]
fcc (1 sublattice, sites: 1, constituents: Fe,Mo,P)	
$L_{Fe,Mo}^{fcc} = (+28,347 - 17.691T)$	[5]
$L_{Fe,P}^{fcc} = (-151,700 + 17T)$	[1]
$L_{Mo,P}^{fcc} = L_{Mo,P}^{bcc}$	E*
$L_{Fe,Mo,P}^{fcc} = (+200,000)$	O*
$Tc^{fcc} = -201x_{Fe}$	[30]
$\beta^{fcc} = -2.1x_{Fe}$	[30]
Mu (μ) (3 sublattices, sites: 7:2:4, constituents: Fe:Mo:Fe,Mo)	
$°G_{Fe:Mo:Fe}^{\mu} = 7°G_{Fe}^{fcc} + 2°G_{Mo}^{bcc} + 4°G_{Fe}^{bcc} + (+39,475 - 6.032T)$	[5]
$°G_{Fe:Mo:Mo}^{\mu} = 7°G_{Fe}^{fcc} + 6°G_{Mo}^{bcc} + (-46,663 - 5.891T)$	[5]
R (3 sublattices, sites: 27:14:12, constituents: Fe:Mo:Fe,Mo)	
$°G_{Fe:Mo:Fe}^{R} = 27 + 14°G_{Mo}^{bcc} + 12°G_{Fe}^{bcc} + (-77,487 - 50.486T)$	[5]
$°G_{Fe:Mo:Mo}^{R} = 27°G_{Fe}^{fcc} + 26°G_{Mo}^{bcc} + (+313,474 - 289.472T)$	[5]
Sigma (σ) (3 sublattices, sites: 8:4:18, constituents: Fe:Mo:Fe,Mo)	
$°G_{Fe:Mo:Fe}^{\sigma} = 8°G_{Fe}^{fcc} + 4°G_{Mo}^{bcc} + 18°G_{Fe}^{bcc} + (-1813 - 27.272T)$	[5]
$°G_{Fe:Mo:Mo}^{\sigma} = 8°G_{Fe}^{fcc} + 22°G_{Mo}^{bcc} + (+83,326 - 69.618T)$	[5]
$L_{Fe:Mo:Fe,Mo}^{\sigma} = (+222,909)$	[5]
Fe$_3$P (2 sublattices, sites: 3:1, constituents: Fe,Mo:P)	
$°G_{Fe:P}^{Fe_3P} = 3°G_{Fe}^{bcc} + °G_{P}^{whi} + (-184,130 - 14.2902T + 8.2245TlnT - 0.007518T^2)$	[1,6](a)
$°G_{Mo:P}^{Fe_3P} = 3°G_{Mo}^{bcc} + °G_{P}^{whi} + (-167,000 + 35T)$	O*
Fe$_2$P (2 sublattices, sites: 2:1, constituents: Fe,Mo:P)	
$°G_{Fe:P}^{Fe_2P} = 2°G_{Fe}^{bcc} + °G_{P}^{whi} + (-170,652 + 3.0174T + 4.5406TlnT - 0.004306T^2)$	[1,6](a)
$°G_{Mo:P}^{Fe_2P} = 2°G_{Mo}^{bcc} + °G_{P}^{whi} + (-204,700 + 45T)$	O*
$L_{Fe,Mo:P}^{Fe_2P} = (-200,000 + 140T)$	O*
Fe$_2$Mo (λ) (2 sublattices, sites: 2:1, constituents: Fe:Mo)	
$°G_{Fe:Mo}^{\lambda} = 2°G_{Fe}^{fcc} + °G_{Mo}^{bcc} + (-10,798 - 0.132T)$	[31]
FeP (2 sublattices, sites: 1:1, constituents: Fe:P)	
$°G_{Fe:P}^{FeP} = °G_{Fe}^{bcc} + °G_{P}^{whi} + (-136,020 - 11.6006T + 6.3362TlnT - 0.005343T^2)$	[1,6](a)
Mo$_3$P (2 sublattices, sites: 3:1, constituents: Mo:P)	
$°G_{Mo:P}^{Mo_3P} = 3°G_{Mo}^{bcc} + °G_{P}^{whi} + (-223,500 + 33.5T)$	O*
MoP (2 sublattices, sites: 1:1, constituents: Mo:P)	
$°G_{Mo:P}^{MoP} = °G_{Mo}^{bcc} + °G_{P}^{whi} + (-219,200 + 45T)$	O*

The thermodynamic data of pure components are taken from Dinsdale [30] unless not shown in the table. Parameter values, except for Tc and β, are in J/mol

O*: Parameter optimized in this work

E*: Parameter estimated in this work

(a) Simplified function. The reference states of Fe and P (HSER) used of Shim et al.[6] have been changed[1] to bcc-Fe and white-P, respectively

Raghavan[13] is observed. Additional calculations, using the data of Gustafsson,[10] have been done for the six vertical sections. They show slightly different phase equilibria and slightly worse agreement with these measurements (for the sake of clarity only the liquidus lines of Gustafsson[10] are plotted in Fig. 6 through 11).

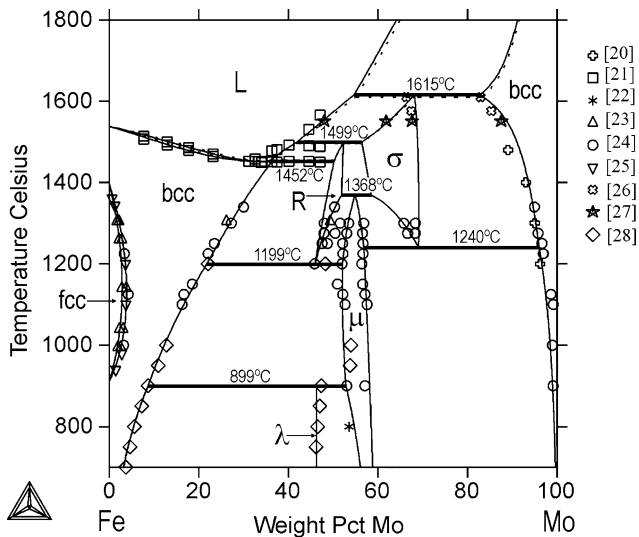In Fig. 13, the phase equilibria suggested by Raghavan[13] at 800 °C (broken lines) agree well with the current

Fig. 1 The Fe-Mo phase diagram calculated with the parameters of Andersson,[5] partially modified in this work, together with experimental data points.[20–28] The solid lines refer to the current calculations and the dotted lines refer to those of Gustafsson[10]
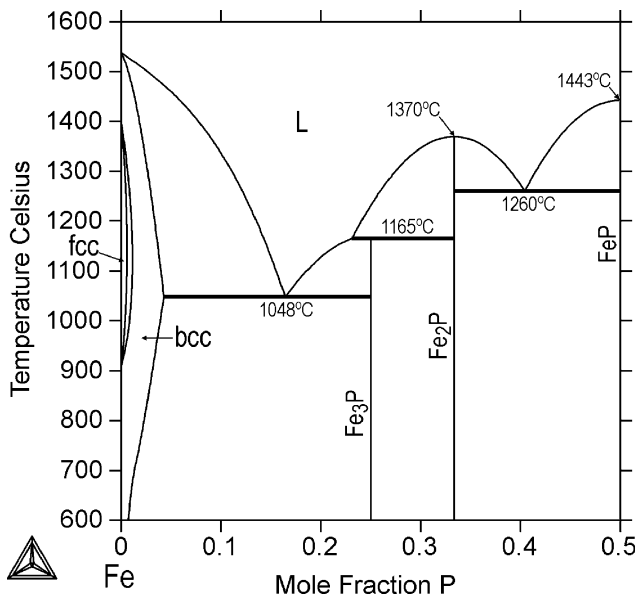

Fig. 2 The Fe-P phase diagram calculated with the parameters of Miettinen and Vassilev.[1] The diagram is identical to that of Shim et al.[6] excluding minor deviations in the bcc- and fcc-regions
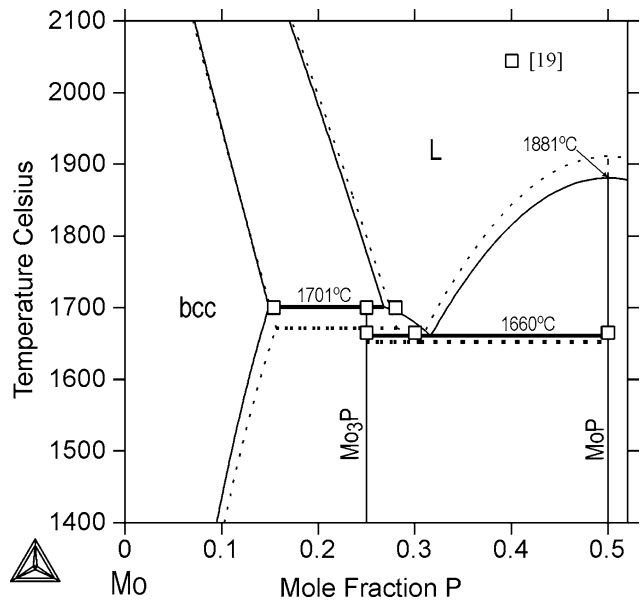

Fig. 3 The Mo-P phase diagram calculated with the parameters obtained in this work, together with the suggested experimental data points of Brewer and Lamoreaux.[19] The solid lines refer to the current calculations and the dotted lines refer to those of Gustafsson[10]
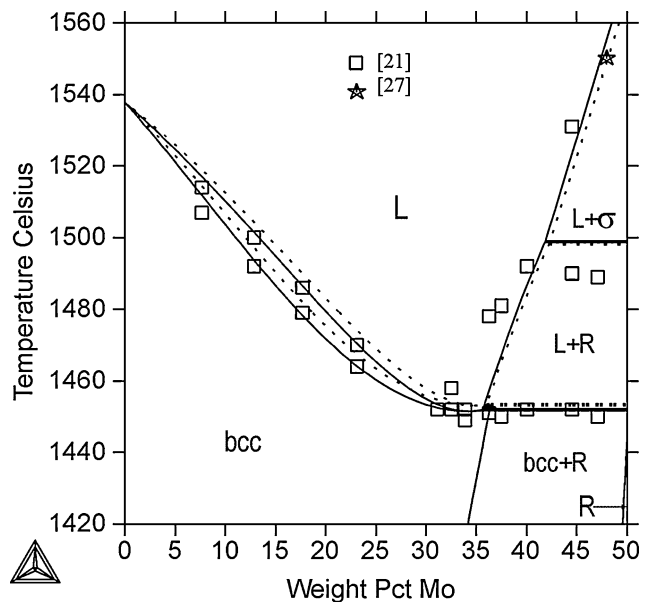

Fig. 4 The Fe-rich side of the Fe-Mo phase diagram calculated with the parameters retained or obtained in this work (solid curves), together with the experimental data points of Gibson et al.[21] and Ichise et al.[27] The dotted curves show the calculations of Gustafsson[10]

calculations but disagree with those of Gustafsson.[10] The 800 °C isotherm has recently been studied also by Olinyuk et al.,[33] who found two ternary compounds, [Fe$_{(1-x)}$-Mo$_{(x)}$]$_2$P (x = 0.18–0.70) and [Fe$_{(1-x)}$Mo$_{(x)}$]$_3$P (x = 0.85–0.90). According to the latter study the former compound overlaps the current (Fe,Mo)$_2$P phase, but does not extend to the nearly binary Fe$_2$P phase. Obviously, the solid state equilibria of the system should be revised as soon as more experimental measurements become available.

Figure 14 illustrates the satisfactory agreement between the calculated (this work) and the experimental (Yamada and Kato[16]) phosphorous activity coefficient (γ_P^{Mo}) in the liquid phase, at 1600 °C. The symbol γ_P^{Mo} is used in order to describe the Mo-content effect on the P-activity coefficient and is defined as: $\gamma_P^{Mo} = \gamma_P^{(Fe-Mo-P)}/\gamma_P^{(Fe-P)}$. In the latter
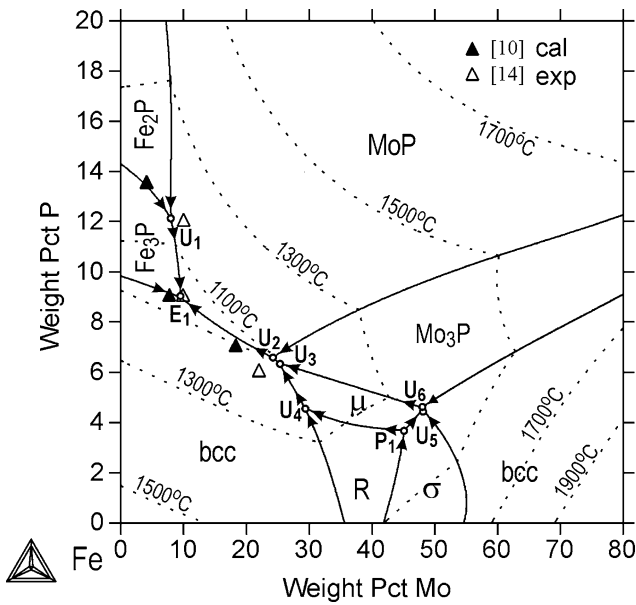
Fig. 5 Liquidus projection of the Fe-Mo-P system calculated with the parameters obtained in this work, together with the experimental data for the invariants from Vogel and Horstmann[14] and the respective values calculated by Gustafsson[10] (see Table 4). The calculated liquidus isotherms between 1100 and 1900 °C (dotted lines) are shown
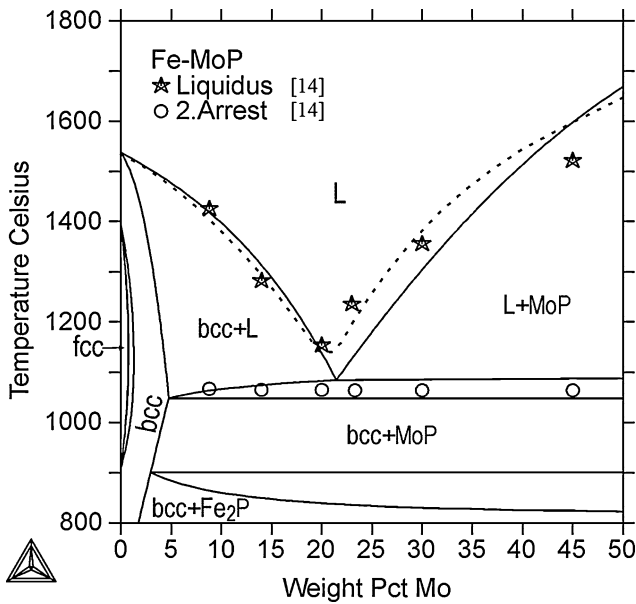

Fig. 7 Calculated vertical section of the Fe-Mo-P system at 5 wt.% P, together with the experimental data of Vogel and Horstmann.[14] The symbol "2.Arrest" is for a thermal arrest. The liquidus, calculated with the parameters of Gustafsson[10] is shown as well (dotted curve)

Fig. 6 Calculated vertical section of the Fe-Mo-P system along the section Fe-MoP, together with the experimental data of Vogel and Horstmann.[14] The symbol "2.Arrest" is for a thermal arrest. The liquidus, calculated with the parameters of Gustafsson[10] is shown as well (dotted curve)

Fig. 8 Calculated vertical section of the Fe-Mo-P system at 10 wt.% P, together with the experimental points of Vogel and Horstmann.[14] The symbol "2.Arrest" is for a thermal arrest. The liquidus, calculated with the parameters of Gustafsson[10] is shown as well (dotted curve)

Ueno et al.[18] derived a theoretical equation using the pseudo-potential formalism coupled with the free energy of a hard sphere system. The P-activity values calculated with this equation agree excellent with the current calculations. All these results point toward negative deviations from the ideal solution behavior. The respective P-activity calculated with the parameters of Gustafsson,[10] (Fig. 14, dotted line) show opposite (i.e., positive) deviations from the Rault's law.

expression the P content (mole fractions) is fixed to $x_P = 0.001$, referring to a very low P-content, applied but not quantified, by Yamada and Kato.[16]
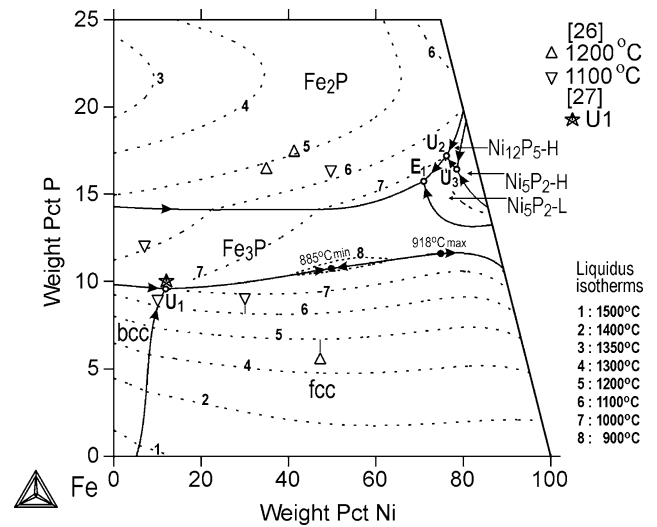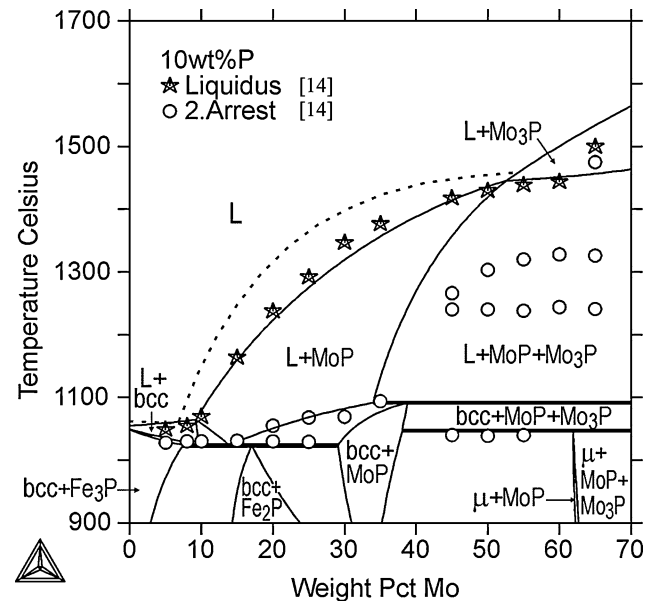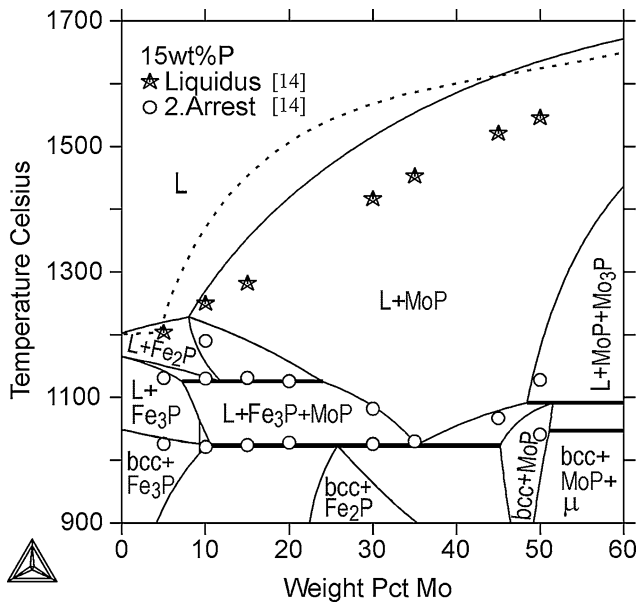
Fig. 9 Calculated vertical section of the Fe-Mo-P system at 15 wt.% P, together with the experimental data of Vogel and Horstmann.[14] The symbol "2.Arrest" is for a thermal arrest. The liquidus, calculated with the parameters of Gustafsson[10] is shown as well (dotted curve)
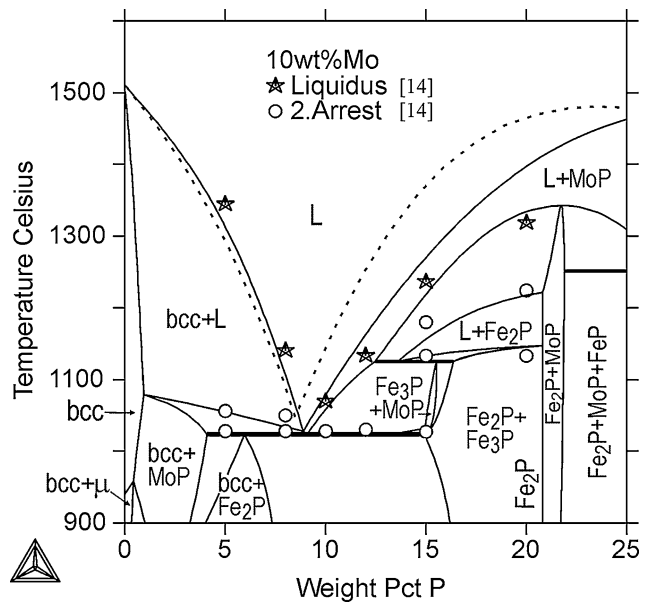

Fig. 11 Calculated vertical section of the Fe-Mo-P system at 10 wt.% Mo, together with the experimental data of Vogel and Horstmann.[14] The symbol "2.Arrest" is for a thermal arrest. The liquidus, calculated with the parameters of Gustafsson[10] is shown as well (dotted curve)
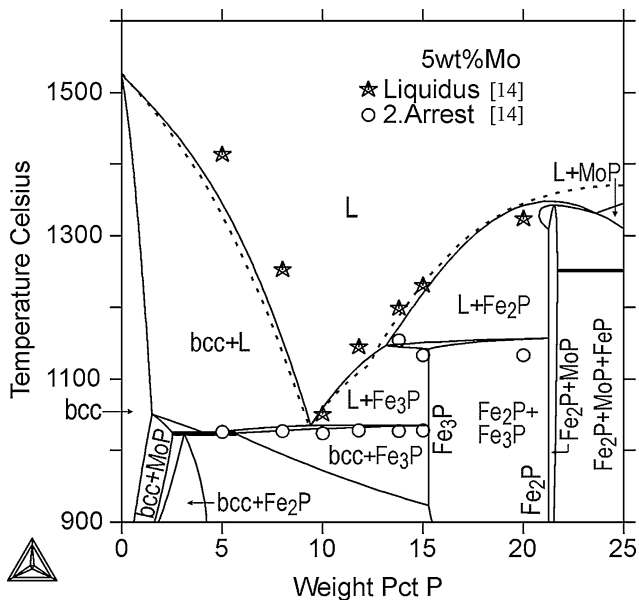

Fig. 10 Calculated vertical section of the Fe-Mo-P system at 5 wt.% Mo, together with the experimental points of Vogel and Horstmann.[14] The symbol "2.Arrest" is for a thermal arrest. The liquidus, calculated with the parameters of Gustafsson[10] is shown as well (dotted curve)
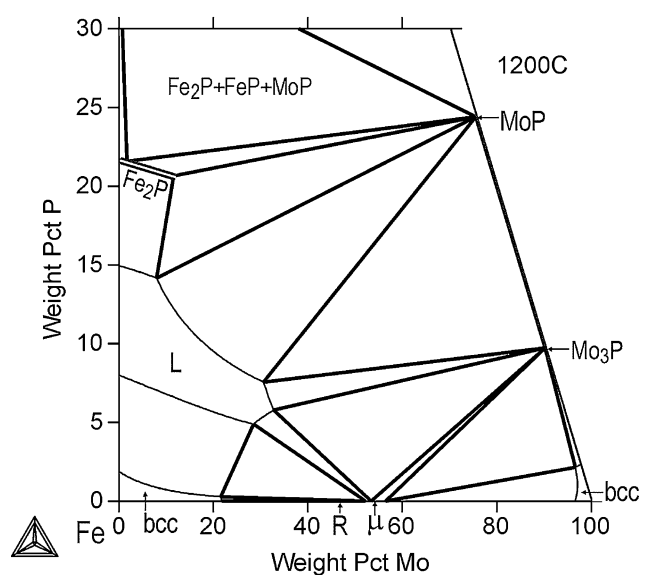
Calculations has also been carried for the parameter $\varepsilon_P^{Mo} = \ln(\gamma_P^{Mo})/x_P$, at 1400 °C, in ternary alloys containing about 20 at.% P. In this case, both assessments (this work

Fig. 12 Isotherm of the Fe-Mo-P system (Fe-rich side) at 1200 °C calculated with the parameters obtained in this work

and Gustafsson[10]), yield a value close to $\varepsilon_P^{Mo} = -2$, whereas the measurements of Ban-ya[17] give that $\varepsilon_P^{Mo} = -7.26$. Such a low value, however, indicates too high stability for the liquid phase so that the calculated (phosphide + liquid phase) equilibria of the present work could not be preserved.
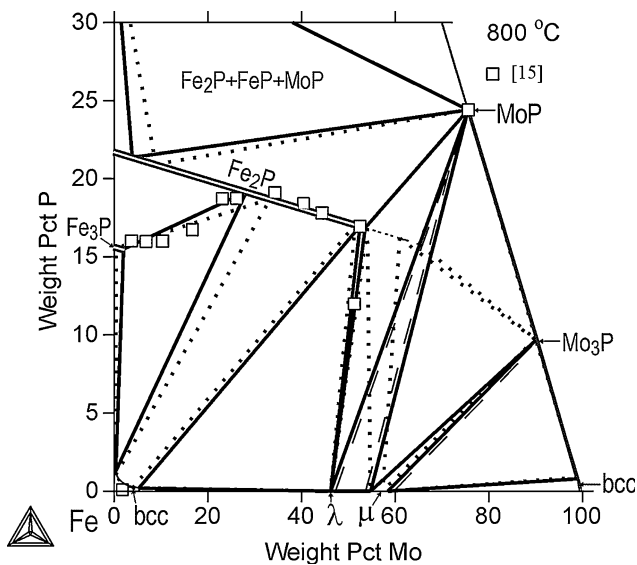
Fig. 13 Calculated isotherm of the Fe-Mo-P system at 800 °C (solid curves), together with the experimental points of Kaneko et al.[15] and some phase equilibria suggested by Raghavan[13] (broken lines). The dotted lines show the results calculated by using the parameters of Gustafsson[10]
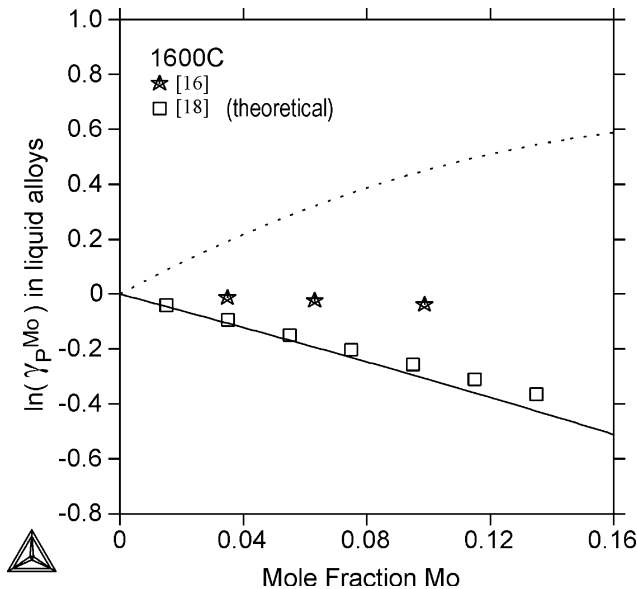

Fig. 14 Calculated P-activity coefficient, γ_P^{Mo}, in liquid Fe-Mo-P alloys at 1600 °C, (solid line) together with experimental (Yamada and Kato[16]) and theoretically assessed (Ueno et al.[18]) data. The dotted line shows the respective activity values up to the calculations of Gustafsson[10]

4. Summary

A thermodynamic reoptimization of the binary subsystem Mo-P has been done. In addition, a slight modification was made for the liquid phase description of the

Table 4 Calculated (this study and Gustafsson[10]) and experimental (Vogel and Horstmann[14]) invariant points and temperatures in the Fe-Mo-P system: t: temperature, °C; Liq and L: liquid phase; E_j: eutectic reaction; P_j: peritectic reaction; U_j: reaction of unclassified type

Reaction	Code	t, °C	Wt.% Mo in Liq	Wt.% P in Liq	Reference
L = bcc + Fe₃P + MoP	E_1	1024	9.5	9.0	This study
		1025	7.7	9.0	[10]
		1023	9.9	9.0	[14]
L + Fe₂P = Fe₃P + MoP	U_1	1125	8.0	12.1	This study
		1141	4.1	13.5	[10]
		1125	10.0	12.0	[14]
L + Mo₃P = bcc + MoP	U_2	1093	24.2	6.6	This study
L + μ = bcc + MoP	U_2	1106	18.3	7.0	[10]
L = μ + bcc + MoP	E_2	1035	22.0	6.0	[14]
L + μ = bcc + Mo₃P	U_3	1104	25.2	6.4	This study
L + R = bcc + μ	U_4	1219	29.3	4.6	This study
L + σ = μ + bcc	U_5	1346	48.1	4.5	This study
L + bcc = μ + Mo₃P	U_6	1341	47.9	4.6	This study
L + σ + R = μ	P_1	1368	45.1	3.7	This study
L = FeP + Fe₂P + MoP	E_3	1251	2.3	27.5	This study

adopted Fe-Mo assessment. Thereafter, a description of the ternary Fe-Mo-P system was obtained.

Thirteen phases (liquid, bcc, fcc, Mu, R, Sigma, Fe₃P (dissolving Mo), Fe₂P (dissolving Mo), Fe₂Mo, FeP, Mo₃P, MoP and (P)) are considered in the current work. Good or reasonable correlation between the calculated and the experimental thermodynamic and phase equilibrium data has been observed. Clear improvement is obtained for the liquid state thermodynamics in regard to the previous optimization of this system. The results of the current optimization have been added to the thermodynamic database on Fe-X-P systems.

References

1. J. Miettinen and G. Vassilev, Thermodynamic Description of Ternary Fe-X-P Systems. Part 1: Fe-Cr-P, *JPED*, 2014, **35**(4), p 458-468
2. J. Miettinen and G. Vassilev, Thermodynamic Description of Ternary Fe-X-P Systems. Part 2: Fe-Cu-P, *JPED*, 2014, **35**(4), p 469-475
3. J. Miettinen and G. Vassilev, Thermodynamic Description of Ternary Fe-X-P Systems. Part 3: Fe-Mn-P, *JPED*, 2014, **35**(5), p 587-594

4. J. Miettinen, S. Louhenkilpi, H. Kytönen, and J. Laine, IDS: Thermodynamic-Kinetic-Empirical Tool for Modeling of Solidification, Microstructure and Material Properties, *Math. Comput. Simulat.*, 2010, **80**, p 1536-1550

5. J.-O. Andersson, A Thermodynamic Evaluation of the Fe-Mo-C System, *CALPHAD*, 1988, **12**, p 9-23

6. J.-H. Shim, C.-S. Oh, and D.N. Lee, Thermodynamic Properties and Calculation of Phase Diagram of the Fe-P System, *J. Korean Inst. Met. Mater.*, 1996, **34**, p 385-393

7. J.-H. Shim, C.-S. Oh, and D.N. Lee, Thermodynamic Assessment of the Fe-C-P System, *Z. Metallkd.*, 2000, **91**, p 114-120

8. H. Ohtani, N. Hanaya, M. Hasebe, S. Teraoka, and M. Abe, Thermodynamic Analysis of the Fe-Ti-P Ternary System by Incorporating First-Principles Calculations into the CALPHAD Approach, *CALPHAD.*, 2006, **30**, p 147-158

9. C. Wu, W. Huang, X. Su, X. Peng, H. Wang, and Y. Liu, Experimental Investigation and Thermodynamic Calculation of the Al-Fe-P System at Low Phosphorus Contents, *CALPHAD*, 2012, **38**, p 1-6

10. P. Gustafsson, Study of the Thermodynamic Properties of the C-Cu-Fe-P, Fe-Mo-P and Fe-Ni-P Systems. Report IM-2549, Institute of Metals Research, Stockholm, 1990

11. H. Lukas, S.G. Fries, and B. Sundman, *Computational Thermodynamics: The Calphad Method*, Cambridge University Press, UK, 2007

12. R. Guerin and M. Sergent, Synthesis and Crystallographic Study of the System MP-MoP and MP-WP (M = 3d Element), *Compt. Rend.*, 1975, **281C**, p 777-780, [in French]

13. V. Raghavan, *Phase Diagrams for Ternary Iron Alloys, Part 3*, Indian Institute of Metals, Calcutta, 1988

14. R. Vogel and D. Horstmann, The Iron-Iron Phosphide-Molybdenum Phosphide-Molybdenum Phase Diagram, *Arch. Eisenhüttenwes.*, 1953, **24**, p 369-374, [in German]

15. H. Kaneko, T. Nishizawa, K. Tamaki, and A. Tanifuji, Solubility of Phosphorus in α and γ Iron, *Nippon Kinzoku Gakkai-Si.*, 1965, **29**, p 166-170, [in Japanese]

16. K. Yamada and E. Kato, Effect of Dilute Concentrations of Si, Al, Ti, V, Cr Co, Ni, Nb and Mo on the Activity Coefficient of P in Liquid Iron, *Trans. Iron Steel Inst. Jpn.*, 1983, **23**, p 51-55

17. S. Ban-Ya, N. Maruyama, and Y. Kawase, Effects of Ti, V, Cr, Mn Co, Ni, Cu, Nb, Mo and W on the Activity of Phosphorus in Liquid Iron, *J. Iron Steel Inst. Jpn.*, 1984, **70**, p 65-72, [in Japanese]

18. S. Ueno, Y. Waseda, K.T. Jacob, and S. Tamaki, Theoretical Treatment of Interaction Parameters in Multicomponent Metallic Solutions, *Steel Res.*, 1998, **59**, p 474-483

19. L. Brewer, R.H. Lamoreaux, Molybdenum: Physico-Chemical Properties of its Compounds, and Alloys. *Vienna: Atomic Energy Review*, Special Issue No. 7, L. Brewer, Eds. IAEA, Vienna, 1980

20. J.L. Ham, An Introduction to Arc-Cast Molybdenum and its Alloys, *Am. Soc. Mech. Eng. Trans.*, 1951, **73**, p 723-732

21. W.S. Gibson, J.R. Lee, and W. Hume-Rothery, Liquidus-Solidus Relations in Iron-Rich Iron-Niobium and Iron-Molybdenum Alloys, *J. Iron Steel Inst.*, 1961, **198**, p 64-66

22. R.D. Rawlings and C.A. Newey, Study of the Iron-Molybdenum System by Means of Diffusion Couples, *J. Iron Steel Inst.*, 1968, **206**, p 273-276

23. G. Kirchner, H. Harvig, and B. Uhrenius, Experimental and Thermodynamic Study of the Equilibria between Ferrite Austenite and Intermediate Phases in the Fe-Mo, Fe-W, and Fe-Mo-W Systems, *Metall. Trans.*, 1973, **4**, p 1059-1067

24. C.P. Heijwegen and G.D. Rieck, Determination of the Phase Diagram of the Mo-Fe System Using Diffusion Couples, *J. Less Common Met.*, 1974, **37**, p 115-121

25. P.J. Alberty and C.W. Haworth, The Solubility of Mo in Gamma-Iron, *Met. Sci.*, 1975, **9**, p 140-149

26. Y. Ueshima, E. Ichise, T. Mori, On the Fe-Mo Phase Diagram. *Tetsu-to-Hagane*, 1979, **65**, S-684-6 [in Japanese]

27. E. Ichise, T. Maruo, H. Sasho, Y. Ueshima, and T. Mori, Knudsen Cell-Mass Spectrometric Determination of Activities in Fe-Mo Alloys, *Tetsu-to-Hagane.*, 1980, **66**, p 1075-1083, [in Japanese]

28. T. Takayama, M.Y. Wey, and T. Nishizawa, Effect of Magnetic Transition on the Solubility of Alloying Elements in bcc Iron and fcc Cobalt, *Trans. Jpn Inst. Met.*, 1981, **22**, p 315-325

29. Y. Iguchi, S. Nobori, K. Saito, and T. Fuwa, A Calorimetric Study of Heats of Mixing of Liquid Alloys Fe-Cr, Fe-Mo, Fe-W, Fe-V, Fe-Nb, Fe-Ta, *J. Iron Steel Inst. Jpn.*, 1982, **68**, p 633-640, [in Japanese]

30. A.T. Dinsdale, SGTE Data for Pure Elements, *CALPHAD.*, 1991, **15**, p 317-425

31. Z.-P. Jin and C. Qiu, An Experimental Study and Thermodynamic Evaluation of the Fe-Mo-Ti System at 1000°C, *Metall. Trans. A*, 1993, **24A**, p 2137-2142

32. J.-O. Andersson, T. Helander, L. Höglund, P. Shi, and B. Sundman, Thermo-Calc & DICTRA, Computational Tools for Materials Science, *CALPHAD.*, 2002, **26**, p 273-312

33. A.O. Olinyuk, Y.F. Lomnytska, M.V. Dzevenko, S.S. Stoyko, and A. Mar, Phase Equilibria in the Fe-Mo-P System at 800 °C and Structure of Ternary Phosphide $(Mo_{1-x}Fe_x)_3P$ $(0.10 < x < 0.15)$, *Inorg. Chem.*, 2013, **52**, p 983-991